

# Synthesis and Characterization of Heat-Resistant *N*-Phenylmaleimide–Styrene–Maleic Anhydride Copolymers and Application in Acrylonitrile–Butadiene–Styrene Resin

Chenyang Zhao,<sup>1</sup> Jianting Dong,<sup>1</sup> Suming Li,<sup>2</sup> Zhongyong Fan<sup>1</sup>

<sup>1</sup>Department of Materials Science, Fudan University, Handan Road No. 220, Shanghai 200433, People's Republic of China

<sup>2</sup>Max Mousseron Institute of Biomolecules, Unité Mixte de Recherche (France) Centre National de la Recherche Scientifique 5247, Faculty of Pharmacy, University Montpellier I, Montpellier 34060, France

Received 28 August 2011; accepted 27 November 2011

DOI 10.1002/app.36544

Published online in Wiley Online Library (wileyonlinelibrary.com).

**ABSTRACT:** The heat-resistant copolymer of *N*-phenylmaleimide (NPMI)–styrene (St)–maleic anhydride (MAH) was synthesized in xylene at 125°C with di-*tert*-butyl diperoxyterephthalate as an initiator. The characteristics of the copolymer were analyzed by Fourier transform infrared spectroscopy, nuclear magnetic resonance spectroscopy (<sup>1</sup>H-NMR and <sup>13</sup>C-NMR), gel permeation chromatography, and elemental analysis. The <sup>13</sup>C-NMR results show that the copolymer possessed random sequence distribution; this was also supported by the differential scanning calorimetry experiment, in which a single glass-transition temperature (*T*<sub>g</sub>) of 202.3°C was observed. The thermal stability and degradation mechanism of the copolymer were investigated by thermogravimetric analysis.

Using the Kissinger equation and Ozawa equation, we proved a nucleation controlling mechanism with an apparent activation energy of 144 kJ/mol. Blends of acrylonitrile–butadiene–styrene with the NPMI–St–MAH copolymer with various contents were prepared with a twin-screw extruder processes. The mechanical and thermal properties of the materials, such as the tensile and flexural strength, *T*<sub>g</sub>'s, and Vicat softening temperatures, were all enhanced with the addition of the modifier, whereas the melt flow index decreased. © 2012 Wiley Periodicals, Inc. *J Appl Polym Sci* 000: 000–000, 2012

**Key words:** blends; copolymers; mechanical properties; thermal properties

## INTRODUCTION

The polymerization behavior of *N*-phenylmaleimide (NPMI) has stimulated considerable interest because of its special structure. The polymer chain contains a five-membered planar ring and a strong polar carbonyl group; these hinder the rotation of the backbone chain and result in greater structural stiffness and higher thermal stability. However, because of the steric interference and electrostatic repulsion between the monomers, it is difficult to get homopolymers of NPMI with a high molecular weight.<sup>1</sup> The high glass-transition temperature (*T*<sub>g</sub>) of poly(*N*-phenylmaleimide) [poly(NPMI)] also leads to difficulty in processing. One of the modification methods for resolving these problems is copolymerization.<sup>2–4</sup>

The copolymerization of NPMI and styrene (St) has been reported in many articles.<sup>5,6</sup> The copolymers had close to an alternating chain structure, independent of the monomer feed molar fractions and the copolymerization methods. It was also found

that although the homopolymerization of NPMI was an equilibrium reaction with a ceiling temperature of about 76°C, the copolymerization of NPMI and St took place in an alternating fashion, regardless whether the NPMI monomer concentration was above or below its equilibrium concentrations.<sup>7</sup> The monomer reactivity ratios [*r*<sub>1</sub> = 0.0530 (St) and *r*<sub>2</sub> = 0.0256 (NPMI)] were obtained by the Mayo–Lewis equation, and the strong tendency for alternation was proved.<sup>8</sup>

It is known that a charge-transfer complex (CTC) participates in the copolymerization process of St and NPMI.<sup>9</sup> Several approaches based on the expected formation of CTC have been proposed to treat the kinetic data of this system. Seiner and Litt<sup>10</sup> first derived a mathematical formulation for this alternating system. Because of the complexity of the expressions, it can only be used under certain restrictions, which in most cases do not represent the real situation. Shirota et al.<sup>11</sup> proposed a treatment of the data based on an assumption that the alternating structure is formed because of the stabilization of the transition state in the cross reactions of the complex and the monomers. Pan et al.<sup>12</sup> presented a new kinetic model with the assumption of a homopropagation and cross-propagation and a

Correspondence to: Z. Fan (zyfan@fudan.edu.cn).

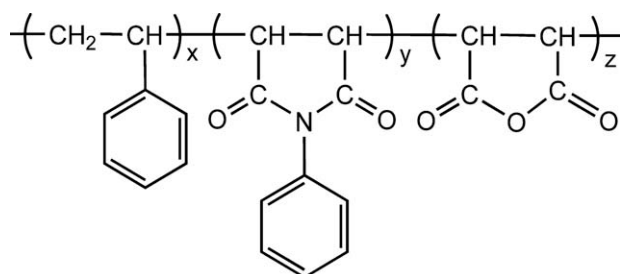


**Figure 1** Chemical structure of the NPMI-St-MAH copolymer.

diffusion-controlled termination. The initial rate of copolymerization was measured as a function of the monomer molar ratios, and the participation of the CTC and the free monomers was quantitatively estimated.

However, because of its poor compatibility with the acrylonitrile-butadiene-styrene (ABS) matrix, the NPMI-St alternating copolymer was not effective in improving the heat resistance of ABS. The tendency for phase separation during the blending process led to an unexpected impact strength. On the contrary, the NPMI-St random copolymer with a constant composition and random sequence distribution overcame these disadvantages<sup>13</sup> and resulted in a better combination between the thermal, mechanical, and rheological properties.

Generally, the formation of CTC is mainly affected by two factors.<sup>14</sup> One is the control of the reaction at a relatively high temperature; the other is the use of polar solvents. These two methods can reduce the tendency toward alternation and, therefore, lead to relatively random sequence distributions. The relative reactivity ratios of the monomers, NPMI and St, were found to be solvent-related, depending on the dielectric constant and the polarity of the solvent.<sup>15</sup> However, because of restrictions of the boiling point and the solubility of the solvents, it is difficult to control the copolymer structure simply by changing the solvents. As a result, the optimization of the processing temperature becomes the most effective way to obtain a random copolymer product.

In addition, several patents<sup>16,17</sup> have described that when the maleimide copolymers are employed for the preparation of composite materials, structures that involve the anhydride units have better compatibility with the resin matrix and enhance the notch sensitivity of the material considerably. Therefore, for the free-radical copolymerization of NPMI with St here, maleic anhydride (MAH) was selected as a third monomer to adjust the properties and the structure of the copolymer. The predicted chemical structure of the copolymer is shown in Figure 1.

In this study, the NPMI-St-MAH copolymer was synthesized at 125°C with di-*tert*-butyl diperoxyter-

ephthalate as an initiator. The product was characterized by Fourier transform infrared (FTIR) spectroscopy and nuclear magnetic resonance (NMR) spectroscopy. The effect of the sequence distribution on the thermal properties, such as the  $T_g$  and thermal degradation mechanism, of the copolymer were studied. The blends of ABS resin with NPMI-St-MAH random copolymers were prepared to improve the heat resistance of the materials, and the mechanical and processing properties were also researched.

## EXPERIMENTAL

### Materials

St was purchased from Shanghai Runjie Chemical Reagent Co., Ltd. (Shanghai, China). It was washed with a 5 wt % aqueous sodium hydroxide solution and then with water three times to remove the inhibitor. It was dried over calcium oxide before being distilled under reduced pressures. NPMI was purchased from Fuyang Taian Chemical Co., Ltd. (Hangzhou, China), recrystallized from an ethanol/water mixture (volume ratio = 1 : 2) three times, and then dried before use. The initiator, di-*tert*-butyl diperoxyterephthalate, was supplied by our laboratory. MAH, xylene, acetone, methanol, and pyridine were purchased from Shanghai Lingfeng Chemical Reagent Co., Ltd. (Shanghai, China) and were used as received.

Commercial-grade ABS resin (20/12/68 w/w/w) with a weight-average molecular weight ( $M_w$ ) of 150,000 was provided by Sinopec Shanghai Gaoqiao Petrochemical Corp. (Shanghai, China). Its melting index and density were 16.4 g/10 min and 1.04 g/cm<sup>3</sup>, respectively. A commercialized ABS heat-resistant modifier, Styrene-N-phenylmaleimide (SMI), was purchased from DENKA Denki Kagaku Kogyo Kabushiki (Tokyo, Japan).

### Synthesis of the NPMI-St-MAH copolymer

NPMI (14.7 g), St (26.5 g), MAH (0.84 g), and xylene (140 mL) were added to a 250-mL four-necked flask, which was equipped with a stirrer, a thermometer, a condenser, and a nitrogen duct. The mixture was stirred at 76°C for 40 min before the initiator, di-*tert*-butyl diperoxyterephthalate, was added. The copolymerization was carried out in an oil bath thermostated at 125°C for 4 h under a nitrogen atmosphere and then cooled to room temperature. For purification, the copolymer was dissolved in acetone, and the solution was poured into an excess of methanol to remove the residual monomers and initiator. This procedure was repeated twice. The copolymer obtained was dried *in vacuo* at 60°C to a constant weight, and the weight conversion was determined gravimetrically.

### Titration of the anhydride content

The content of MAH was determined by titration of the acid groups derived from the anhydride functions. After dissolution of 0.5 g of purified copolymer in 50 mL of acetone, 50  $\mu$ L of pyridine and 50  $\mu$ L of deionized water were added to hydrolyze the anhydride functions into carboxylic acid functions. The reaction was maintained at 50°C for 1 h. The carboxylic acid concentration was determined directly by a 0.1 mol/L KOH–ethanol solution with a 0.5 wt % phenolphthalein–ethanol solution as an indicator. The titration was ended when the color change was stable. For comparison, a blank solution was also treated under the same conditions.

### Compounding and specimen preparation

The NPMI–St–MAH copolymer, SMI, and ABS were dried at 90°C for 3 h in a vacuum oven before blending. *N*-Phenylmaleimide–styrene–maleic anhydride (NSM)/ABS and SMI/ABS blends containing 2.5, 5, 10, 15, and 25 wt % modifier were prepared with twin-screw extruder processes. These blends were coded as NSM2.5, NSM5, NSM10, NSM15, and NSM25 and SMI2.5, SMI5, SMI10, SMI15, and SMI25, respectively. The screw speed was 40 rpm, and the melt temperature was 240°C. In this process, 0.4 phr of magnesium stearate and 0.3 phr of 2,6-di-*tert*-butyl-4-methylphenol were introduced as a lubricant and an oxidation inhibitor, respectively. The pelletized materials were injection-molded into various ASTM standard specimens with an injection-molding machine. The injection temperature and pressure were 230°C and 40 MPa, respectively.

### Measurement and characterization

The content of the NPMI was calculated on the basis of the nitrogen content of the copolymer, determined on an Elementar Vario EL3 elemental analyzer (Hanau, Germany). FTIR spectra were obtained on a Nicolet Magna-IR 560 spectrometer (Madison, Wisconsin, US) with a resolution of 2  $\text{cm}^{-1}$  from 4000 to 400  $\text{cm}^{-1}$ . The molecular weight measurement was carried out on a PerkinElmer Series 200 gel permeation chromatography instrument (Waltham, Massachusetts, US) at 40°C with tetrahydrofuran (THF) as the eluent and monodisperse polystyrene as the reference. The  $^1\text{H-NMR}$  and  $^{13}\text{C-NMR}$  spectra were recorded on Bruker DMX500 spectrometer at 400 MHz and a Bruker AMX400 spectrometer (Karlsruhe, Germany) at 100 MHz, respectively. Deuterated chloroform ( $\text{CDCl}_3$ ) was used as the solvent, and tetramethylsilane was used as the internal standard.

The  $T_g$  was measured on a DuPont 910 differential scanning calorimetry (DSC) instrument (Wilmington,

Delaware, US) at a heating rate of 20°C/min with a sample weight of 5 mg in a nitrogen gas flow. The  $T_g$  value was taken from the transition midpoint of the heat capacity on the second run. Thermogravimetric analysis (TGA) was obtained on a DuPont TA 951 thermogravimetric analyzer. The samples were heated at speeds of 5, 10, 15, and 25°C/min, respectively, from room temperature to 600°C under an atmosphere of  $\text{N}_2$ .

The tensile strength was measured on a Sans CMT6104 tensile machine (Shenzhen, China) according to ASTM D 638 with a crosshead speed of 50 mm/min. The flexural properties were conducted on an Instron model 2366 instrument (Norwood, Massachusetts, US). The measurement was carried out according to ASTM D 790 with a loading speed of 3 mm/min. The melt flow index (MFI) values were obtained according to ASTM D 1238 with a S.R.D. RL-11B1 test equipment (Shanghai, China). The testing temperature was 220°C, and the load used was 10 kg. The Vicat softening temperatures (VSTs) of the specimens were determined with a Ceast 6921 machine (Pianezza, Italy). The heating speed and load were 50°C/h and 5 kg, respectively. The density was measured with an A&D GF-300D density balance (Tokyo, Japan) according to ASTM D 792 at room temperature.

## RESULTS AND DISCUSSION

The radical copolymerization of NPMI, St, and MAH resulted in a heterogeneous system because of the insolubility of the NPMI–St–MAH copolymer into xylene. After purification, a colorless powder was obtained with an average conversion of more than 75%. The  $M_w$  and polydispersity index of the resulting copolymer were  $4.6 \times 10^4$  and 2.2, respectively.

Compared to the traditional alternating copolymerization of NPMI–St, which has a maximum yield about 60% when the monomer molar ratio is close to 1 : 1,<sup>18</sup> the yield of the radical copolymerization of NPMI, St, and MAH was much higher and reached up to 80%; this opened up possibilities for large-scale industrial application. In terms of the free-radical copolymerization, the copolymer had a relatively narrow composition distribution with a polydispersity index no greater than 3. This was as expected because the properties of the materials were largely dependent not only on the apparent molecular weight but also on the degree of polydispersity.

### Chemical structure and composition of the NPMI–St–MAH copolymer

The structure of the product was characterized by FTIR spectroscopy, and the major regions of the spectra are depicted in Figure 2. As shown in the picture, the characteristic absorption of the NPMI segments was found to be 1381  $\text{cm}^{-1}$ , which was

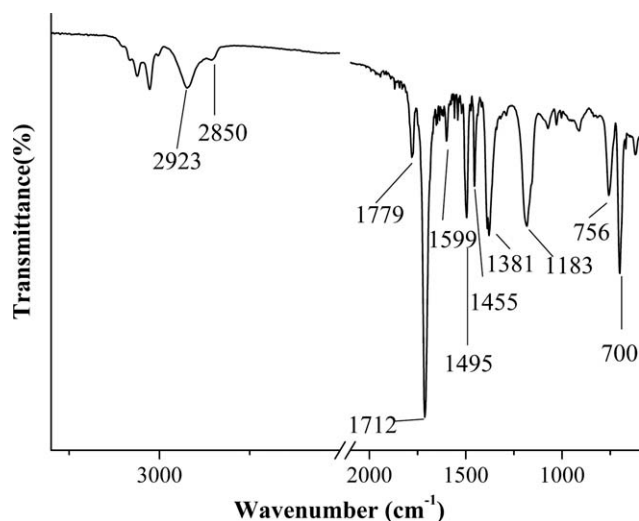


**Figure 2** Typical FTIR spectrum of the NPMI-St-MAH copolymer.

indicative of a five-membered ring of the imide structure.<sup>19</sup> The appearance of bands at 1712 and 1183  $\text{cm}^{-1}$  represented the stretching vibrations of carbonyl and C–N bonds, respectively. The peaks at 1599, 1455, and 1495  $\text{cm}^{-1}$  were associated with the phenyl groups in the NPMI and St units, reflecting the semicircle stretching and mixed C–H bending of a monosubstituted benzene ring. The existence of St moieties was confirmed by the stretching vibrations of  $\text{CH}_2$  at 2923 and 2850  $\text{cm}^{-1}$  without a disturbance of other groups. Another typical absorption, at 1779  $\text{cm}^{-1}$ , belonged to the C=O of MAH fragments; this peak revealed that the MAH monomers were successfully polymerized in the polymer chain. Therefore, these analyses evidenced the formation of the NPMI-St-MAH copolymer. The absence of absorption bands at 926, 1235, and 1790  $\text{cm}^{-1}$  indicated that the copolymer was free from poly(maleic anhydride) structures.<sup>20,21</sup>

Furthermore, the content of each component was established quantitatively. The weight fraction of MAH was calculated according to the following equation:

$$\text{MAH}(\%) = [(V_1 - V_0)C_{\text{KOH}}M/2000 m] \times 100\% \quad (1)$$

where  $C_{\text{KOH}}$  is the concentration of the KOH-ethanol solution (mol/L),  $m$  is the sample weight (g),  $V_1$  and  $V_0$  are the volumes added to the sample and the blank solution, respectively, and  $M$  is the molecular weight of MAH (98.06).

On the basis of the results of elemental analysis and chemical titration, the St, NPMI, and MAH contents were calculated to be 61.5 : 35.5 : 3 in molar ratio and 51 : 47 : 2 in weight ratio, respectively. It is known that the copolymer composition has a close relationship with its physical properties. The NPMI-

St copolymer showed a considerable increase in the thermal stability with increasing NPMI content.<sup>2</sup> However, in the case of preparing a highly heat-resistant copolymer using maleimide monomers, although it was necessary to have more than a certain amount of NPMI, we found the resultant product to be poor in both the impact resistance and fluidity when the amount was increased excessively. Therefore, the monomer composition of NPMI to be charged to the copolymerization had to be adjusted within a certain range, 28–55%, depending on the actual conditions.<sup>16</sup> The compatibility of the copolymer was largely dependent on the St and MAH contents. The interfacial energy with ABS was sufficiently low when the MAH content was about 2 wt %.<sup>22</sup>

Copolymers with the same molecular weights and compositions may vary in their sequence distributions. The sequence information can be best obtained by means of  $^{13}\text{C}$ -NMR spectroscopy because  $^{15}\text{N}$ -NMR spectra in many cases are difficult to interpret, whereas  $^1\text{H}$ -NMR spectra are not sensitive to sequence effects, although they are useful in certain aspects.<sup>23</sup>

The  $^1\text{H}$ -NMR and  $^{13}\text{C}$ -NMR spectra of the NPMI-St-MAH copolymer fit well into this picture. The  $^1\text{H}$ -NMR spectra up to 400 MHz did not give sequence information but were useful in determining the molar ratios of the monomer units. The molar ratio of NPMI to St as measured by  $^1\text{H}$ -NMR was 1 : 1.8 (Fig. 3); this was in agreement with the elemental analysis results. The  $^{13}\text{C}$ -NMR spectrum of the NPMI-St-MAH copolymer is shown in Figure 4. It is clear that the absorption of double bonds, 133.7 ppm from =CH in the NPMI units<sup>1</sup> and 114.7 ppm from =CH<sub>2</sub> in the St units, disappeared; this

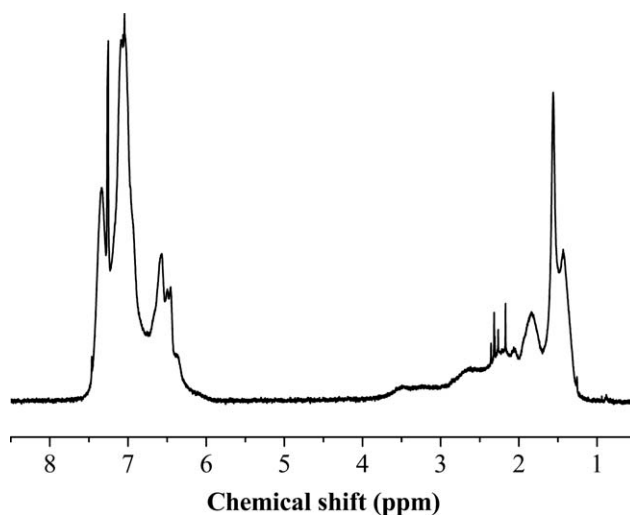


**Figure 3**  $^1\text{H}$ -NMR spectrum of the random NPMI-St-MAH copolymer {1.2–2.4 ppm, CH and CH<sub>2</sub> in the St monomer unit; 2.4–3.8 ppm, CH in the imide ring; 6.2–7.1 ppm, CH in Phenyl(St); 7.1–7.6 ppm, CH in Phenyl(NPMI);  $n_{\text{NPMI}}:n_{\text{St}} = [A_{\delta(2.4 \sim 3.8)} + A_{\delta(7.1 \sim 7.6)}/7]:[A_{\delta(1.2 \sim 2.4)} + A_{\delta(6.2 \sim 7.1)}/8]$ }.

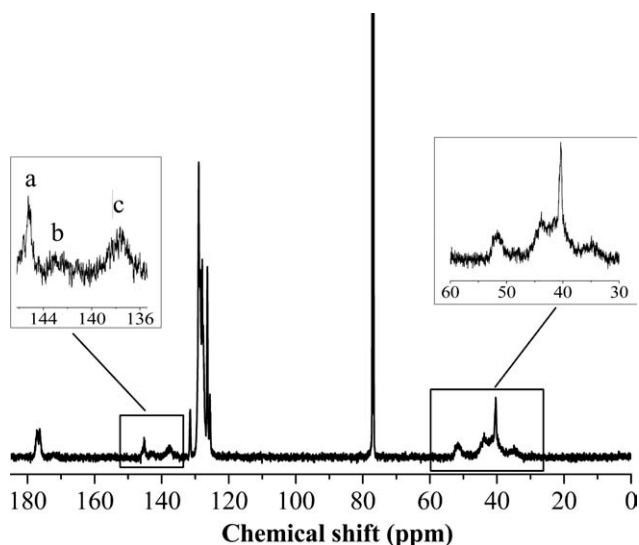


**Figure 4**  $^{13}\text{C}$ -NMR spectrum of the random NPMI-St-MAH copolymer.

indicated that the polymerization proceeded through the opening of the double bonds. The signals assigned to carbonyl were observed at 176.4 and 177.3 ppm. These belonged to the NPMI and MAH units, respectively. The absorptions of the phenyl carbons in NPMI and St units appeared to be between 126 and 132 ppm. The broadened signal at 30–55 ppm was assigned to substituted methyl in the backbone of the copolymer. The broadening of methylene and methylidene carbon peaks may have reflected the complexity of the configuration of the polymer main chain. No remarkable side reactions, such as carbonyl addition or the ring opening of the imide group, were observed. This was probably because the electron density on the  $\text{C}=\text{C}$  double bond was significantly reduced by the electron-withdrawing effect of the carbonyl groups, and the electrophilicity of carbonyl carbons became lower because of the cyclic imide structure.<sup>24</sup>

Furthermore, it was reported that there was no absorption from 130 to 144 ppm in the  $^{13}\text{C}$ -NMR spectrum of polystyrene and no absorption from 132 to 170 ppm for the poly(NPMI) and poly(maleic anhydride) either.<sup>25</sup> So the band appearance at 133–144 ppm was brought about by the interactions between different units and could be regarded as useful information for distinguishing the triads.

The carbon assignments in the range 130–145 ppm are given in Table I. The capital letters S and M stand for St and NPMI/MAH, respectively. As expected,<sup>26</sup> the quaternary aromatic next to the polymer chain carbon  $\text{Ph}(\text{C}^1)$  of St units was proven to be sensitive to the St-centered triad sequence distribution. The homogeneous structure of St, SSS, appeared at 145.3 ppm. Because of the shielding effect of NPMI/MAH units on the  $\text{Ph}(\text{C}^1)$  of St, the

MSS/SSM and MSM sequences shifted downfield by 1.8 and 7.7 ppm, respectively. The NPMI/MAH-centered triad sequence, SMS, shifted downfield by 13.8 ppm at the most. The NPMI and MAH units are treated equivalently here because of their similar chemical structures and almost the same shielding effect on the resonance of the  $\text{Ph}(\text{C}^1)$  of the St units.<sup>27</sup> The MAH was as polar as NPMI and only less conjugative (lower in reactivity) than NPMI.

The existence of different triad sequences justified a random structure of the copolymer that was obtained from solution copolymerization by the selection of the proper reaction temperature and initiator and monomer ratios. Studies of the sequence distribution may also reveal the mechanism of this copolymerization process. From the assignment of the triads, the free-radical attacking site and the propagation reaction of copolymerization could be inferred.<sup>25</sup> As shown by  $^{13}\text{C}$ -NMR, there was no M-M structure in the polymer chain. The absence of SMM, MMS, and MMM triad sequences indicated that the NPMI free radicals could not attack the NPMI monomers in the chain propagation reaction.

#### Thermal properties of the NPMI-St-MAH copolymer

As a promising heat-resistant modifier, the NPMI-St-MAH random copolymers have received much interest, not only in its synthesis but also in its thermal properties. The  $T_g$  values of the NPMI-St-MAH copolymer were measured by DSC, and the thermogram is illustrated in Figure 5. It was clear that only one  $T_g$  of 202.3°C could be observed; this indicated a relatively homogeneous structure of the copolymer. This finding was different from that in a previously reported work in which the NPMI-St copolymer was produced via emulsion copolymerization. That copolymer with the same NPMI content showed two different  $T_g$ 's by DSC, corresponding to polystyrene and poly(styrene-*alt*-*N*-phenylmaleimide) [poly(St-*alt*-NPMI)], respectively.<sup>28</sup> The discrepancy could be easily explained by the fact that  $T_g$  was dependent not only on the composition of the polymer but also on its sequence distribution.

In the conventional copolymerization of electron-donor monomers (St) and electron-acceptor monomers

**TABLE I**  
Carbon Assignments of the  $^{13}\text{C}$ -NMR Spectra for the NPMI-St-MAH Copolymer Triads

Peak number	Chemical shift (ppm)	Assignments
a	145.3	$\text{Ph}(\text{C}^1)$ , SSS
b	143.5	$\text{Ph}(\text{C}^1)$ , MSS+SSM
c	137.6	$\text{Ph}(\text{C}^1)$ , MSM
	131.5	$\text{Ph}(\text{C}^1)$ , SMS

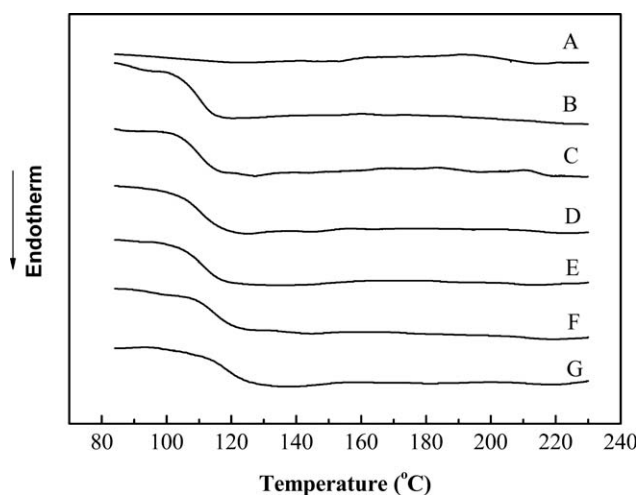


**Figure 5** DSC curves of the (A) NPMI-St-MAH copolymer, (B) virgin ABS resin, (C) NSM2.5, (D) NSM5, (E) NSM10, (F) NSM15, and (G) NSM25.

(NPMI/MAH), which is controlled exclusively by the polar effect, because of the large difference of polarity between the monomers, St and NPMI/MAH have a strong tendency to complex and form an alternating structure rather than a random or homogeneous one. Thus, a cross-propagation process dominates in the first stage of copolymerization until the NPMI/MAH concentration becomes too low, and then, the remaining St starts to homopolymerize. The final product, with high conversion, is a mixture of polystyrene and poly(*N*-phenylmaleimide/maleic anhydride-*alt*-styrene). This explains the appearance of double  $T_g$ 's. However, when the temperature rises to 125°C, the growth of CTC decreases, and the activity of St increases. As a result, random copolymerization, which is controlled by a balanced combination of general reactivity and polar effects, is supposed to occur. Compared with the  $T_g$  of polystyrene ( $107 \pm 2^\circ\text{C}$ ),<sup>29</sup>  $T_g$  of the NPMI-St-MAH copolymer was much higher and reached up to 202.3°C, although it was still lower than the  $T_g$  of the completely alternating structure (230°C).<sup>5</sup> This indicated a nonalternating sequence distribution and was in agreement with the analysis of <sup>13</sup>C-NMR.

Next, the relationship between the  $T_g$  of the random copolymer and the  $T_g$  of the component homopolymers was considered. The Fox equation<sup>30</sup> is based on free volume concepts and is expressed as follows:

$$1/T_g = \sum W_i/T_{gi} \quad (2)$$

where  $T_{gi}$  and  $T_g$  represent the glass-transition temperatures of the homopolymers and the corresponding copolymers, respectively, and  $W_i$  is the weight fraction of the monomer unit. In this work, 503 and 380 K were used for the  $T_g$ 's of poly(NPMI-*alt*-St)

and the atactic formed polystyrene, respectively. The slight differences in the reported  $T_g$  values were probably due to the different thermal histories, molecular weights, sample sizes, and so on.<sup>29</sup> Because MAH is only 2 wt % and has a comparable  $T_g$  with NPMI when copolymerized alternately with St,<sup>31</sup> it was treated as the NPMI for simplification.

Because of the participation of CTC, the  $T_g$  was calculated with the Fox equation with a CTC weight fraction of 81% and an St weight fraction of 19%. The  $T_g$  obtained was highly consistent with the DSC results with a  $\Delta T_g$  of 3°C. The establishment of this assumption indicated that under copolymerization conditions of 125°C with a weakly polar solvent, the enhanced reactivity of St led to a lower tendency for alternation, despite the fact that the formation of CTC was unavoidable. As a result, the CTC monomer copolymerized with St randomly, as was evident from the <sup>13</sup>C-NMR and DSC measurements. The deviation between the Fox equation prediction and the DSC measurement may have resulted from the strong polarity of carbonyl groups, which decreased the mobility of the polymer chain. Also, the similar molecular structures of the monomers also led to tight chain packing and reduced the free volumes of the copolymer.

On the basis of the previous discussions, the propagation reactions of NPMI/St/MAH copolymerization can be written as follows:



where the free monomers and CTC equilibrium are related as follows:



The homopolymerizations of NPMI and MAH, which were not detected from FTIR spectroscopy and <sup>13</sup>C-NMR, will not happen:<sup>25</sup>



TGA is a widely used technique because it can, in many cases, determine the upper limit use temperatures of a material. The thermal stability of the NPMI-St-MAH copolymer could be arbitrarily defined as a function of the initial weight loss/decomposition temperature ( $T_i$ ) and the maximum decomposition rate temperature ( $T_m$ ) at particular heating rates under the atmosphere of N<sub>2</sub>. The nonisothermal thermogravimetry curves recorded from room temperature to 600°C are shown in Figure 6, together with their first derivatives (differential thermogravimetry).

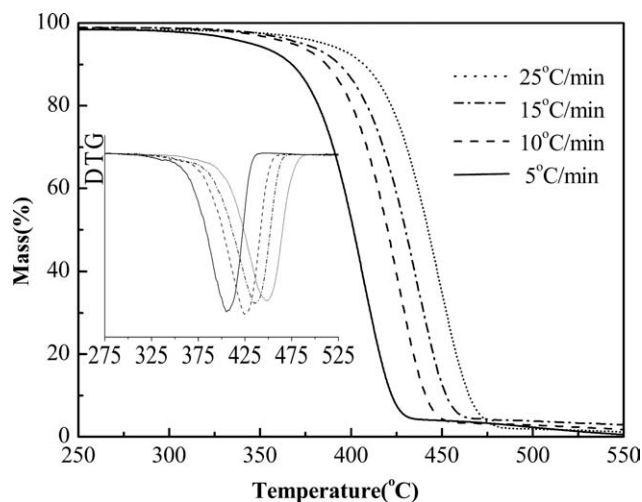


**Figure 6** TGA curves for the thermal degradation of the NPMI-St-MAH copolymer at heating rates of 5, 10, 15, and 25 °C/min under an N<sub>2</sub> atmosphere. The inset shows the first derivative of the TGA curves (differential thermogravimetry).

As shown in the picture, the thermogravimetry curves were C types<sup>32</sup> and corresponded to a single-stage decomposition process. The copolymer showed excellent thermal stability, in that it had no weight loss below 290 °C; this temperature was much higher than the processing temperature of ABS, which is about 220–240 °C in most cases.

For comparison,  $T_i$ ,  $T_m$ , and the residual mass ( $W$ ) at 600 °C are summarized in Table II. The experimental data varied accordingly with different heating rates.  $T_m$  increased about 40 °C with an improvement of 20 °C/min in the heating speed, whereas the residue diminished about 2 wt % at 600 °C. At the same heating speed of 10 °C/min, the  $T_i$  value (302 °C) was between those of poly(NPMI) (364 °C)<sup>1</sup> and atactic polystyrene (275 °C),<sup>33</sup> as expected. The significant enhancement in  $T_i$ , which was about 30 °C as compared to polystyrene, could be attributed to the existence of five-membered planar rings and strong polar carbonyl groups, which improved the potential barrier of molecular motion. The onset decomposition was supposed to occur in polystyrene-rich microdomains, so  $T_i$  would increase with the increasing NPMI content. However, the difference between  $T_m$  of the NPMI-St-MAH copolymer and that of poly(NPMI) (435 °C) was not obvious.

TGA measurement also provides a practical approach for determining the reaction mechanism of the thermal degradation process. Kinetic parameters, that is, the apparent activation energy and reaction order ( $n$ ), can be extracted from dynamic data by various methods.

All kinetic studies assume that the isothermal rate of weight loss ( $d\alpha/dt$ ) is a linear function of a temperature-dependent rate constant ( $k$ ) and a tempera-

ture-independent function of weight loss  $f(\alpha)$ , that is

$$d\alpha/dt = kf(\alpha) \quad (8)$$

where  $f(\alpha)$  depends on the decomposition mechanism.

If  $k$  is replaced by the Arrhenius equation, a basic equation for kinetic studies can be obtained:

$$d\alpha/dT = A/\beta f(\alpha) \exp(-E/RT) \quad (9)$$

where  $A$  is the pre-exponential factor and is assumed to be independent of temperature,  $E$  is the apparent activation energy,  $T$  is the absolute temperature,  $R$  is the gas constant, and  $\beta$  ( $dT/dt$ ) is the heating speed.

The Kissinger method<sup>34</sup> is a widely used differential method that has a good reproducibility because it adopts the inflection temperatures as the basis for determining the kinetic parameters. It is expressed as a derivation of eq. (2):

$$\ln(\beta/T_m^2) = \{\ln(AR/E) + \ln[n(1 - \alpha_m)^{n-1}]\} - E_\alpha/(RT_m) \quad (10)$$

where  $E_\alpha$  is the apparent activation energy at corresponding weight loss ratios and  $\alpha_m$  is the weight loss ratio corresponding to  $T_m$ .

By analyzing the changes brought about by variations in heating rate, we calculated the apparent activation energy from a plot of  $\ln(\beta/T_m^2)$  versus  $1000/T_m$ , which had a slope of  $(-E_\alpha/R)$ . Figure 7 shows the fitting plot treated by this method. An apparent activation energy of 144 kJ/mol was obtained, as listed in Table II. We noticed that the apparent activation energy of the NPMI-St-MAH copolymer was not only lower than the corresponding value of poly(NPMI), which was 199.5 kJ/mol according to Kissinger's procedure,<sup>35</sup> but was also inferior to that of polystyrene (156 kJ/mol).<sup>36</sup> A possible explanation for this deviation was that the polystyrene had a much higher molecular weight ( $M_w = 3\text{--}4 \times 10^5$ ) and degree of tacticity, which increased the intermolecular interaction. This increment promoted the energy of the transition state and led to a relatively higher apparent activation energy.

**TABLE II**  
Results Calculated from the Kissinger and Ozawa Equations

Heating rate (°C/min)	$T_i$ (°C)	$T_m$ (°C)	$W$ (%)	Kissinger (kJ/mol)	$\alpha$ (%)	Ozawa (kJ/mol)
5	291	406	0.53	144	5	135
10	302	426	1.78		10	145
15	314	437	2.92		15	148
25	317	449	2.20		20	151

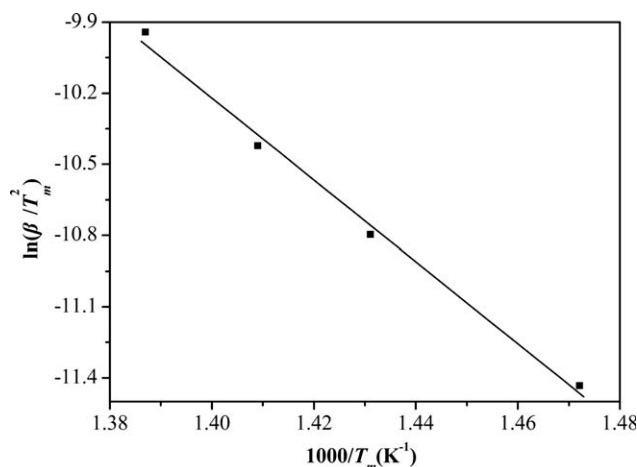


**Figure 7** Kissinger method applied to the experimental data at different heating rates.

In contrast, the Ozawa method<sup>37</sup> is an integral method used to determine the apparent activation energy for a given weight loss ratio. After an integration of eq. (2) is taken with the Doyle approximation,<sup>38</sup> the logarithmic result is written as

$$\ln \beta = \ln\{0.0048AE_{\alpha}/[g(\alpha)R]\} - 1.0516E_{\alpha}/(RT) \quad (11)$$

where  $g(\alpha)$  is an integral function of the weight loss ratio.

Because of the Doyle approximation, only relatively low conversions are available to this method. The plots of  $\ln \beta$  versus  $1000/T$  at given weight loss ratios (5, 8, 11, and 14%) are given in Figure 8. It can be seen from Figure 8 that nearly parallel fitting lines were acquired; this indicated good applicability for this system within the range studied. This fact also indicated that a single mechanism was crucial for the decomposition process.<sup>32</sup> The activation energies obtained corresponding to different weight loss ratios are listed in Table II. A mean value of 145 kJ/mol was acquired; this was in good agreement with the result calculated by eq. (10). As shown in Table II, the apparent activation energy increased with the increment of weight loss ratios. A lower value (135 kJ/mol) in the early stage ( $\alpha < 5\%$ ) may have been due to the prior scission of weak bonds, such as end groups or polystyrene segments. It also showed that the  $E_{\alpha}$  corresponding to the 8% conversion was very close to the value obtained with the Kissinger method.

Compared to other mathematical approximation methods, the Kissinger and Ozawa methods present a clear advantage, in that the apparent activation energy can be determined without previous knowledge of the thermodegradation mechanism. The fact that similar results were obtained from these two different methods indicated that they were reliable for checking the reaction mechanism.

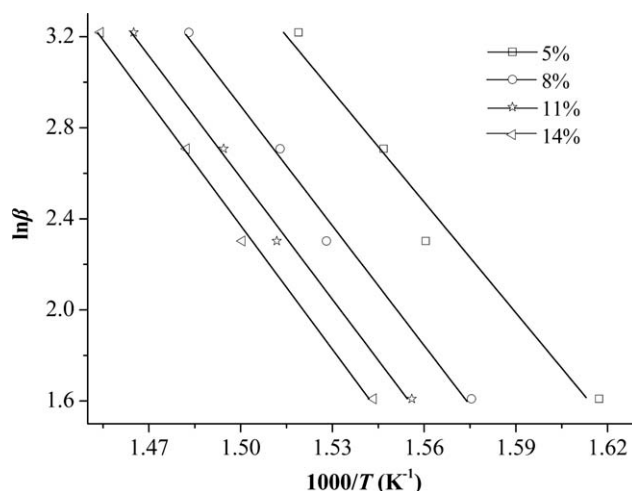


**Figure 8** Plot of  $\log \beta$  against  $1000/T$  at various conversion values in the range 5–14% in steps of 3%.

The degradation mechanism is always characterized as a function of  $n$ . To determine the value of  $n$ , the Crane equation was used:<sup>39</sup>

$$d(\ln \beta)/d(1/T_m) = -E_a/(nR) - 2T_m \quad (12)$$

when  $E_a/(nR) \gg 2T_m$ , it can be simplified as follows:

$$d(\ln \beta)/d(1/T_m) = -E_a/(nR) \quad (13)$$

Thus, a plot of  $\ln \beta$  versus  $1000/T_m$  held for a straight line with a slope of  $(-E_a/nR)$ . With the apparent activation energy taken from the Kissinger equation,  $n$  can be easily calculated when the fitting plot has the maximum linear correlation coefficient. The plot is shown in Figure 9 with an  $n$  of 0.94 and a correlation coefficient of  $-0.9972$ .

Generally, a solid-state process consists of nucleation, growth of the germ, advance of the reaction

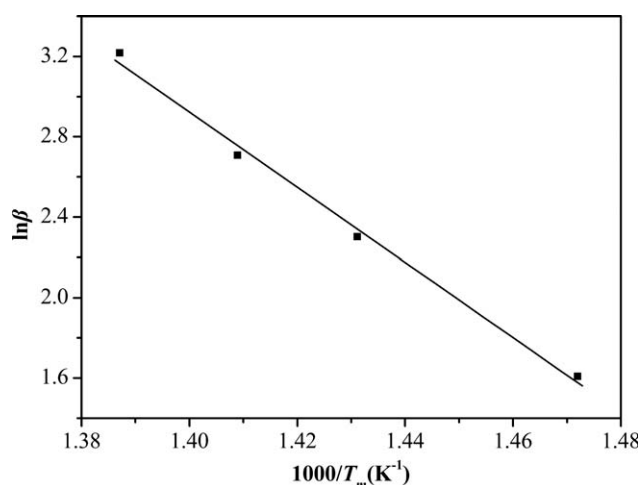


**Figure 9** Plot of  $\ln \beta$  against  $1000/T_m$  with a slope of  $-E_a/nR$ .



**TABLE III**  
**Mechanical and Thermal Properties of the NSM/ABS and SMI/ABS Blends**

Blend material	Tensile strength (MPa)	Flexural strength (MPa)	Flexural modulus (MPa)	Density (g/cm <sup>3</sup> )	VST (°C)	MFI (g/10 min)
ABS	50.9	62.7	2240	1.04	97.6	16.4
NSM2.5	51.1	61.3	2280	1.04	98.8	16.3
NSM5	51.2	60.9	2270	1.05	99.8	14.7
NSM10	51.5	62.1	2370	1.05	102.7	13.9
NSM15	52.2	62.8	2390	1.06	106.4	11.4
NSM25	61.9	72.2	2692	1.07	111	9.4
SMI2.5	51.4	61.1	2275	1.04	99	15.5
SMI5	51.2	60.8	2265	1.04	100	14.8
SMI10	52.2	61.5	2290	1.05	102.9	14.1
SMI15	52.4	62.9	2350	1.06	105.8	12.2
SMI25	55.3	65.8	2470	1.07	113	9.7

interface, diffusion of the product, and so on.<sup>32</sup> The  $n$  obtained was not an integer, which suggested that a combination of several mechanisms occurred during the decomposition process simultaneously/successively. However, the value was close to 1; this indicated that a nucleation mechanism dominated the nonisothermal degradation process and was consistent with the previous conclusions of the Ozawa equation. In addition, it was reported<sup>27</sup> that the degradation order of the NPMI–St copolymer changed from 2 to 1.1 when the molar fraction of NPMI was increased from 0 to 0.51; this perhaps indicated a change in the degradation mechanism as a result of a variation in the copolymer compositions.

#### Physical properties of the NPMI–St–MAH/ABS blends

A series of blends containing different NPMI–St–MAH/ABS ratios were prepared with twin-screw extruder processes. The pelletized materials were injection-molded into various ASTM standard specimens. For comparison, a commercialized ABS heat-resistant modifier was also treated under the same conditions.

The physical properties of the NPMI–St–MAH/ABS and SMI/ABS blends are presented in Table III. The NPMI–St–MAH/ABS blends illustrated better flexural strength and modulus values than the SMI/ABS series for the whole range of compositions studied, especially when the NPMI–St–MAH content was higher than 10 wt %. Compared to those of the virgin ABS resin, the flexural strength and modulus of NSM25 increased by 15 and 20%, respectively. On the other hand, the tensile strength remained almost the same at lower NPMI–St–MAH contents. However, when the proportion of added NPMI–St–MAH exceeded 10%, the tensile strength was greatly enhanced. The NSM25 specimen showed a much higher tensile strength than that of SMI25 by 6.6

MPa. The increment in the tensile and flexural properties may have been due to the rigid character of the NPMI–St–MAH random copolymer; this reduced the deformation at break and hardened the polymer blends. In the case of density, these two series of blends showed similar results for the same composites. The density increased slightly with an increase in modifier content.

VST is a widely employed parameter for quality control and material development in industry. It could be taken as the material's ultimate use point for a short period of time. As shown in Table III, the VST of virgin ABS was only 97.6°C; this restricts its applications in automobiles and domestic appliances. However, the VST value increased more than 0.5°C with the addition of 1 wt % NPMI–St–MAH. The VSTs of NSM10 and NSM15 reached 102.7 and 106.4°C and met the standards of Volkswagen TL527A (100°C) and TL527B (106°C), respectively. These modified ABS resins could be used for interior car fittings and car audio stereo systems, which require good heat resistance to prevent any shape distortion due to heat. In addition, the  $T_g$  values of the NSM/ABS blends and the virgin ABS resin are shown in Figure 5.  $T_g$  improved from 110 to 118°C with increasing NPMI–St–MAH content; this was consistent with the VST results. It should be noted that there was only one  $T_g$  observed for each blend; this indicated a good compatibility between the NPMI–St–MAH random copolymer and the ABS resin matrix.

Processability is one of the most attractive properties of ABS resins. As the NPMI–St–MAH content was increased from 0 to 25 wt %, the MFI values decreased from 16.4 to 9.4 g/10 min; this indicated an increment in the viscosity. The reduction in MFI may have occurred because the NPMI–St–MAH granules retained their shape and functioned as rigid particulate fillers when they were processed and restricted the melt flow.

## CONCLUSIONS

First, NPMI–St–MAH random copolymers were synthesized at 125°C with a solution–precipitation method. The sequence distribution was verified by <sup>13</sup>C-NMR and DSC, which revealed the existence of varied triad sequences and a single  $T_g$  of 202.3°C, which was between those of the homopolymer of St (102°C) and the alternating copolymer of NPMI–St (230°C). Second, the influence of the polymer structure on its thermal stability was assessed by TGA. From different kinetic models (the Kissinger and Ozawa equations),  $E_\alpha$  was confirmed to have a value of 144 kJ/mol. The overall thermodegradation order, calculated from the Crane equation, showed that a nucleation and growth mechanism dominated the depolymerization process. Finally, a series of modified ABS resins based on the NPMI–St–MAH random copolymer were prepared in compositions of 100/0, 97.5/2.5, 95/5, 90/10, 85/15, and 75/25 w/w. These blends showed an excellent balance of physical properties.  $T_g$  and VST increased remarkably with increasing amount of modifier without any affects on the tensile and flexural properties.

## References

- Matsumoto, A.; Kubota, T.; Otsu, T. *Macromolecules* 1990, 23, 4508.
- Barrales-Rienda, J. M.; Gonzalez De La Campa, J. I.; Gonzalez Ramos, J. *J Macromol Sci Pure Appl Chem* 1977, 11, 267.
- Li, A. L.; Lu, J. *J Appl Polym Sci* 2009, 114, 2469.
- Liu, Y. C.; Xu, W.; Xiong, Y. Q.; Zhang, F.; Xu, W. *J Mater Lett* 2008, 62, 1849.
- Lu, Y. B.; Sun, W. L.; Shen, Z. Q. *Eur Polym J* 2002, 38, 1275.
- Cheng, H. T.; Zhao, G. Q.; Yan, D. Y. *J Polym Sci Part A: Polym Chem* 1992, 30, 2181.
- Iwatsuki, S.; Kubo, M.; Wakita, M.; Matsui, Y.; Kanoh, H. *Macromolecules* 1991, 24, 5009.
- Shan, G. R.; Weng, Z. X.; Huang, Z. M.; Pan, Z. R. *J Appl Polym Sci* 1997, 63, 1535.
- Huang, W. Y.; Pan, H. L.; Jiang, B. B.; Ren, Q.; Zhai, G. Q.; Kong, L. Z.; Zhang, D. L.; Chen, J. H. *J Appl Polym Sci* 2011, 119, 977.
- Seiner, J. A.; Litt, M. *Macromolecules* 1971, 4, 308.
- Yoshimura, M.; Nogami, T.; Yokoyama, M.; Mikawa, H.; Shirota, Y. *Macromolecules* 1976, 9, 211.
- Shan, G. R.; Huang, Z. M.; Weng, Z. X.; Pan, Z. R. *Macromolecules* 1997, 30, 1279.
- Jar, P.-Y. B.; Wu, R. Y.; Kuboki, T.; Takahashi, K.; Shinmura, T. *J Appl Polym Sci* 1999, 71, 1543.
- Yao, Z.; Li, B. G.; Cao, K.; Pan, Z. R. *J Appl Polym Sci* 1998, 67, 1905.
- Mohamed, A. A.; Jebrael, F. H.; Elsabee, M. Z. *Macromolecules* 1986, 19, 32.
- Tsuneshige, Y.; Kimura, A.; Toyooka, Y.; Kajimura, K. U.S. Pat. 5,140,067 (1992).
- Fan, Z. Y.; Hu, Y. M.; Dong, J. T.; Lu, Q.; Sun, M.; Bu, H. S. *Chin. Pat.* 101824115A (2010).
- Liu, G. D.; Li, X. C.; Zhang, L. C.; Qu, X. W.; Liu, P. G.; Yang, L. T.; Gao, J. G. *J Appl Polym Sci* 2002, 83, 417.
- Ishida, H.; Wellinghoff, S. T.; Baer, E.; Koenig, J. L. *Macromolecules* 1980, 13, 826.
- De Roover, B.; Sclavons, M.; Carlier, V.; Devaux, J.; Legras, R.; Momtaz, A. *J Polym Sci Part A: Polym Chem* 1995, 33, 829.
- Qiu, W. L.; Hirotsu, T. *Macromol Chem Phys* 2005, 206, 2470.
- Jar, P.-Y. B.; Creagh, D. C.; Konishi, K.; Shinmura, T. *J Appl Polym Sci* 2002, 85, 17.
- Kricheldorf, H. R.; Mang, T.; Jonte, J. M. *Macromolecules* 1984, 17, 2173.
- Hagiwara, T.; Shimizu, T.; Someno, T.; Yamagishi, T.; Hamana, H.; Narita, T. *Macromolecules* 1988, 21, 3324.
- Shan, G. R.; Weng, Z. X.; Huang, Z. M.; Pan, Z. R. *J Appl Polym Sci* 2000, 77, 2581.
- Ha, N. T. H. *Polymer* 1990, 40, 1081.
- Ha, N. T. H.; Fujimori, K.; Craven, I. E. *Macromol Chem Phys* 1997, 198, 3507.
- Yuan, Y.; Siegmann, A.; Narkis, M.; Bell, J. P. *J Appl Polym Sci* 1996, 61, 1049.
- Rieger, J. J. *Therm Anal Calorim* 1996, 46, 965.
- Fox, T. G. *Bull Am Phys Soc* 1956, 1, 123.
- Wästlund, C.; Maurer, F. H. *J Polymer* 1998, 39, 2897.
- Núñez, L.; Fraga, F.; Núñez, M. R.; Villanueva, M. *Polymer* 2000, 41, 4635.
- Brandrup, J.; Immergut, E. H.; Grulke, E. A. *Polymer Handbook*; Wiley: New York, 1999.
- Kissinger, H. E. *Anal Chem* 1957, 29, 1702.
- Sivasamy, P.; Vijayakumar, C. T.; Lederer, K.; Kramer, A. *Thermochim Acta* 1992, 208, 283.
- Ravanetti, G. P.; Zini, M. *Thermochim Acta* 1992, 207, 53.
- Ozawa, T. B. *Chem Soc Jpn* 1965, 38, 1881.
- Doyle, C. D. *Nature* 1965, 207, 290.
- Crane, L. W.; Dynes, P. J.; Kaelble, D. H. *J Polym Sci Part C: Polym Lett* 1973, 11, 533.